Intrinsic Fatigue Crack Propagation in Aluminum–Lithium Alloys: the Effect of Gaseous Environments

ROBERT S. PIASCIK and RICHARD P. GANGLOFF
Department of Materials Science, University of Virginia, Charlottesville, VA 22901, USA

ABSTRACT

Gaseous environmental effects on intrinsic fatigue crack growth are significant for the Al-Li-Cu alloy 2090, peak aged. For both moderate ΔK-low R and low ΔK-high R regimes, crack growth rates decrease according to the environment order: purified water vapor, moist air, helium and oxygen. Gaseous environmental effects are pronounced near threshold and are not closure dominated. Here, embrittlement by low levels of H_2O (ppm) supports hydrogen embrittlement and suggests that molecular transport controlled cracking, established for high ΔK-low R, is modified near threshold. Localized crack tip reaction sites or high R crack opening shape may enable the strong environmental effect at low levels of ΔK. Similar crack growth in He and O_2 eliminates the contribution of surface films to fatigue damage in alloy 2090. While 2090 and 7075 exhibit similar environmental trends, the Al-Li-Cu alloy is more resistant to intrinsic corrosion fatigue crack growth.

KEYWORDS

Aluminum alloy; Al-Li; fatigue crack growth; fracture mechanics; corrosion fatigue; gaseous environment; hydrogen embrittlement; surface film; crack closure.

INTRODUCTION

The objective of this research is to characterize and understand intrinsic fatigue crack propagation in advanced aluminum - lithium based alloys, with emphasis on the damage mechanisms for environmentally assisted transgranular cracking.

Al-Li alloys such as 2090 and 8090 exhibit outstanding fatigue crack propagation resistance, but attributable to the extrinsic effects of crack surface closure contact and crack tip deflection (Venkateswara Rao et al., 1988). Extrinsic crack growth resistance is likely to be geometry, orientation and loading history dependent; thus complicating mechanistic understanding and defect tolerant predictions. The intrinsic fatigue crack

growth (FCG) rate is that which is governed by crack tip chemical and mechanical driving forces, independent of external influences of closure, deflection and bulk chemical factors.

Electrical potential monitoring of physically short (0.3 to 5 mm) fatigue cracks, with programmed stress intensity range (ΔK) and stress ratio (R), successfully yielded intrinsic crack growth kinetics for high strength aluminum alloys (Piascik and Gangloff, 1988a). Application of these methods to alloy 2090 in aqueous chloride electrolytes evidenced good corrosion fatigue resistance relative to alloy 7075, a potentially important effect of surface films and a notable lack of classical hydrogen embrittlement (Piascik and Gangloff, 1988b). The current work examines corrosion fatigue in purified gaseous environments to further understand these damage mechanisms.

EXPERIMENTAL PROCEDURE

Two high strength aluminum alloys, Al-Li-Cu-Zr alloy 2090 and Al-Zn-Mg-Cu alloy 7075-T651 rolled to plate, were studied in the unrecrystallized peak aged condition. Compositions, heat treatment, microstructure and mechanical properties are summarized in Table 1. The crystallographic texture of alloy 2090 is similar to that reported by Yoder et al., (1987); precipitate structures are equivalent to those analyzed by Cassada et al., (1987).

Table 1. Material Properties

Chemical Composition (WT %):

ALLOY 2090 (3.8 cm thick plate)

Li	Cu	Zr	Fe	Si	Mn
2.14	2.45	0.09	0.05	0.04	0.00
Mg	**Cr**	**Ni**	**Ti**	**Na**	**Zn**
0.00	0.00	0.00	0.01	0.001	0.01

ALLOY 7075 (6.4 cm thick plate)

Zn	Mg	Cu	Cr	Zr	Fe
5.74	2.31	1.58	0.20	0.01	0.26
Si	**Mn**	**Ni**	**Ti**	**Na**	**Ca**
0.10	0.05	0.01	0.05	0.000	0.0001

Mechanical Properties: (Long-Transverse,Peakaged)

	Yield	Ultimate
ALLOY 2090	496 MPa	517 MPa
ALLOY 7075 (T651)	466 MPa	540 MPa

Alloy 2090 Material Condition:
Solution treated, water quenched and stretched.
Peakaged 190°C - 4 hrs

Alloy 2090 Microstructure:
Grain size - 3.3 mm (trans.); 0.11 mm (short trans.)
Subgrain size - 15 μm (trans.); 5 μm (short trans.)

Fatigue crack propagation experiments were conducted with single edge notched (SEN) specimens (10.16 mm wide, 2.54 mm thick, 0.25 or 0.89 mm notch depth) machined in the L-T orientation at 1/3 plate thickness. The growth of short cracks, sized between 0.3 and 5 mm, was monitored continuously by a

direct current electrical potential method including 8 to 12 amps current, 0.1 μV potential measurement resolution, 3 μm crack length resolution and an analytical calibration relation (Gangloff, 1982). Long crack compact tension (CT) experiments, with compliance monitoring, were conducted in accordance with ASTM E647, (1988).

Specimens were stressed cyclically (sine wave) with a 44.5 kN servohydraulic test frame at a frequency of 5 Hz in load control. By computer measurement and feedback control, ΔK was maintained constant over segments of growing crack length (0.5 to 1 mm), with step reductions in constant ΔK at constant K_{max} producing increasing stress ratio (R) (Piascik and Gangloff, 1988a). A single specimen characterizes intrinsic and transient to steady state corrosion fatigue crack growth rates for the moderate ΔK Paris regime and for near threshold at high R (namely, ripple loading) (Gao et al., 1988, Crooker et al., 1987). For CT specimens, continuously decreasing ΔK for constant R or K_{max} is accomplished by established methods with controlled shedding rate, C (Saxena et al., 1978, Herman et al., 1988). Crack growth rates (da/dN) are calculated by linear regression analysis of crack length (a) versus load cycles (N) data for constant ΔK and by secant methods for continuously decreasing ΔK. Out of plane cracking, common to Al-Li alloys was not produced by the short crack method.

Fatigue experiments in static gaseous environments; including 2 kPa helium, 20 kPa oxygen and 2 kPa water vapor; were performed in a bakable, metal bellows and gasket-sealed, chamber. Prior to testing, the chamber was evacuated to below 3 μPa and backfilled at low flow with high purity gas (99.998% pure helium or oxygen), further purified by passage through a liquid nitrogen cold trap (Method A). An improved procedure (Method B) was employed for selected experiments. Helium was purified by passage through molecular sieve at 23°C to remove H_2O, followed by a reactive, hot titanium alloy chip getter to further reduce H_2O, O_2 and H_2 contaminants. Fatigue loading times were minimized for this second method to limit environment contamination due to outgassing. A quartz vial, attached to the vacuum chamber and containing distilled water, was used for the water vapor experiments. This water was further purified by repeated (3 times) freezing, evacuation, and boiling. Pressures were measured with a capacitance manometer and specimen temperature was monitored by an attached thermocouple.

RESULTS AND DISCUSSION

Intrinsic Fatigue Crack Growth in Moist Air

The intrinsic fatigue crack growth characteristics of alloy 2090 in moist air (>30% R.H.) are accurately characterized by the short crack, ΔK control method, Fig. 1. Data points (Δ) labeled with R, relate to a short edge crack, less than 4 mm in depth. These seven constant ΔK levels of crack growth were obtained by step increases and decreases in R at a constant K_{max} of 17 $MPa \cdot m^{1/2}$. Crack growth rates were linear for each ΔK segment, without rate transients. Delay retardation was never observed after a ΔK change, due to constant K_{max} and maximum plastic zone size.

Excellent agreement is observed between short crack, constant ΔK-step increased R and long crack, continuously decreasing ΔK constant K_{max} experimental results. Plotted in Fig. 1 are data for a continuously decreasing ΔK experiment at constant K_{max}, conducted with a CT specimen and two K-gradient parameters; $C=-188\ m^{-1}$ for ΔK ranging from 13 $MPa \cdot m^{1/2}$ to 8 $MPa \cdot m^{1/2}$ and $C=-394\ m^{-1}$ for $\Delta K<8\ MPa \cdot m^{1/2}$. Because the experiment was per-

formed at constant K_{max}, the high K-gradient parameter (ASTM E647 recommends $C>-80\ m^{-1}$) does not introduce overload effects causing reduced da/dN. The data in Fig. 1 are in excellent agreement with literature results for alloy 2090 (Piascik and Gangloff, 1988a, Herman et al., 1988).

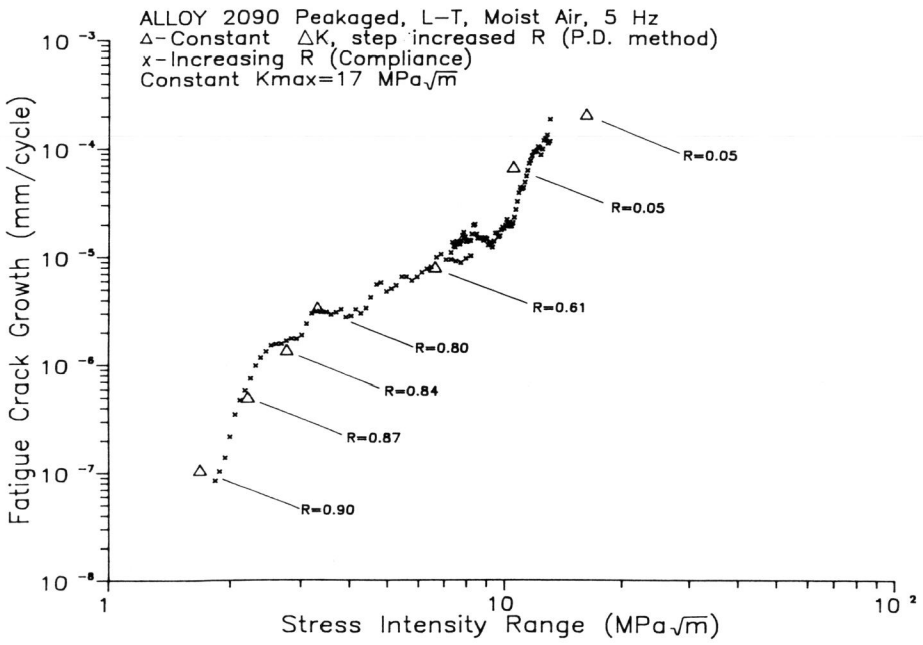

Fig. 1. The intrinsic fatigue crack growth behavior of alloy 2090 in moist air.

Because opening loads were not measured for short crack specimens, compliance based experiments were performed using long crack SEN specimens (38.1 mm wide, 5.0 mm thick, 5.0 mm notch depth) to demonstrate that intrinsic rates of crack growth are measured at low ΔK. For cracks ranging from 5 mm to 13 mm in depth, interfering closure was not observed for R greater than 0.5 and over the ΔK regimes represented in Fig. 1. It is therefore unlikely that closure affects the growth rates of short cracks (< 5 mm) for R greater than 0.6 and ΔK less than 7 $MPa \cdot m^{1/2}$. Roughness induced closure may occur during the moderate ΔK (R=0.05) experiments shown in Fig. 1. Severe deflected crack growth is observed, increasing the likelihood for crack wake closure if Mode II displacements occur. Notably, however, minimal closure was reported for peakaged alloy 2090 at ΔK greater than 9 $MPa \cdot m^{1/2}$ and R=0.1 (Venkateswara Rao et al., 1988).

FCG in Controlled Gaseous Environments

FCG of Alloy 7075 in Gaseous Environments. Fig. 2 contains the results of short crack experiments performed with alloy 7075 in water vapor, helium (purified by Method A), and oxygen. At moderate cyclic stress intensity and low R, a factor of three increase in da/dN is observed in water vapor compared to helium, and oxygen retards fatigue crack growth by a factor of two compared to helium. These results agree with previous findings; dashed lines in Fig. 2 (Gao et al., 1988); where accelerated crack growth was observed for water vapor followed by argon, vacuum, and oxygen. Accelerated growth in water vapor is consistent with hydrogen embrittlement (Gao et al., 1988) and retarded crack growth in oxygen may be caused by oxide induced crack closure, however, surface film effects have not been ruled out. The roles of crack tip rewelding in vacuum and of slip dispersion and irreversibility for oxide covered surfaces remain speculative. Since physically adsorbed He or Ar molecules minimize each process and favor reversible crack tip deformation, such gases provide a reference basis for plastic deformation dominated fatigue damage.

At low ΔK, increased crack growth rate is correlated to the presence of water vapor. The results shown in Fig. 2 reveal accelerated crack growth in 2 kPa water vapor followed by a slight reduction in da/dN for helium and a factor of five reduction in crack growth rate for oxygen compared to water vapor. Notably, the water vapor and helium results exhibit similar crack growth rates compared to moist air, the shaded area in Fig. 2. Here, the upper bound represents intrinsic fatigue crack growth results from microstructural small crack experiments (Lankford and Davidson, 1986) and the lower bound is from high R, long crack experiments (Herman et al., 1988). These rates are significantly faster than crack growth in vacuum.

Petit and coworkers suggest that near-threshold fatigue crack growth in H_2O contaminated nitrogen is rapid relative to dynamic vacuum and similar to moist air due to hydrogen embrittlement (Petit and Zeghloul, 1988). Closure corrected compact tension results in Fig. 2 show accelerated crack growth for nitrogen containing 3 ppm H_2O compared to vacuum. (For vacuum, the upper bound represents results from short crack experiments and the lower bound is the result of closure corrected compact tension measurements.) This acceleration of cracking in N_2/H_2O is consistent with current data for alloy 7075-T651 in Fig. 2. The He environment, purified by Method A, contained between 1 and 5 ppm water due to ineffective cold trap purification and chamber and specimen outgassing. It is not clear why low levels of water vapor are embrittling, because low pressure H_2O molecule transport from the bulk environment to the crack tip may be insufficient to support hydrogen production (Gao et al., 1988). Petit did not consider this kinetic factor when claiming near threshold hydrogen embrittlement in dilute water vapor. We evaluate this consideration for alloy 2090.

Retarded da/dN for oxygen, under closure free high R conditions, suggests that crack tip oxide films mitigate fatigue damage by either precluding contaminant based hydrogen production or by affecting slip processes. The relationship between purely inert gas crack growth rates and values for O_2 must be characterized to resolve the effect of surface films. Such data are obtained for Al-Li alloy 2090, and the competing effects of hydrogen and film formation are examined.

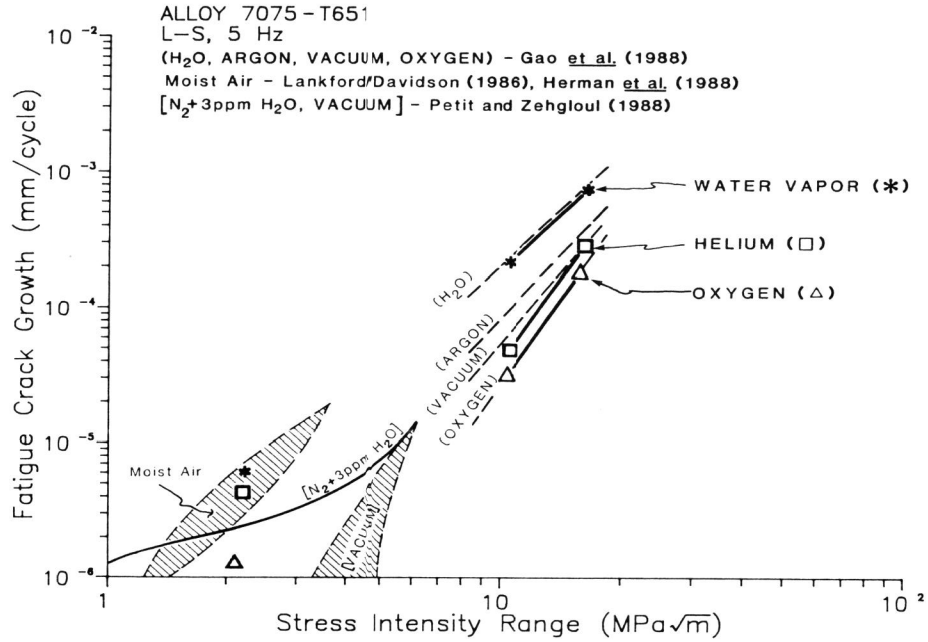

Fig. 2. The fatigue crack growth behavior of alloy 7075-T651 in gaseous environments.

FCG of Alloy 2090 in Gaseous Environments. Shown in Fig. 3 are the results of short crack experiments on alloy 2090 in water vapor, helium (purified by Method B), oxygen, and moist air. At moderate ΔK, da/dN for helium, oxygen and water vapor are equal and only slightly greater than moist air. Retarded fatigue crack growth, a maximum reduction by a factor of five at 11 MPa·$m^{1/2}$, is observed for oxygen. Constant ΔK results plotted in Figs. 2 and 3 represent intrinsic crack growth, not considered in previous studies. At moderate ΔK and low R, extrinsic effects are minimized by short crack lengths and closure free crack growth is ensured by evaluating each constant ΔK experiment for constant da/dN.

Increased crack growth rate in alloy 2090 is correlated to the presence of water vapor for near threshold loading, similar to 7075. At low ΔK and high stress ratio, results in Fig. 3 reveal that 2 kPa H_2O produces the fastest growth followed by moist air. Equal factors of eight reduction in da/dN are observed for helium and oxygen compared to pure water vapor. A comparison of moist air results with the accelerated fatigue crack growth observed for water vapor and the retarded da/dN for oxygen suggests a complex water vapor/oxygen environmental effect for alloy 2090 in moist air.

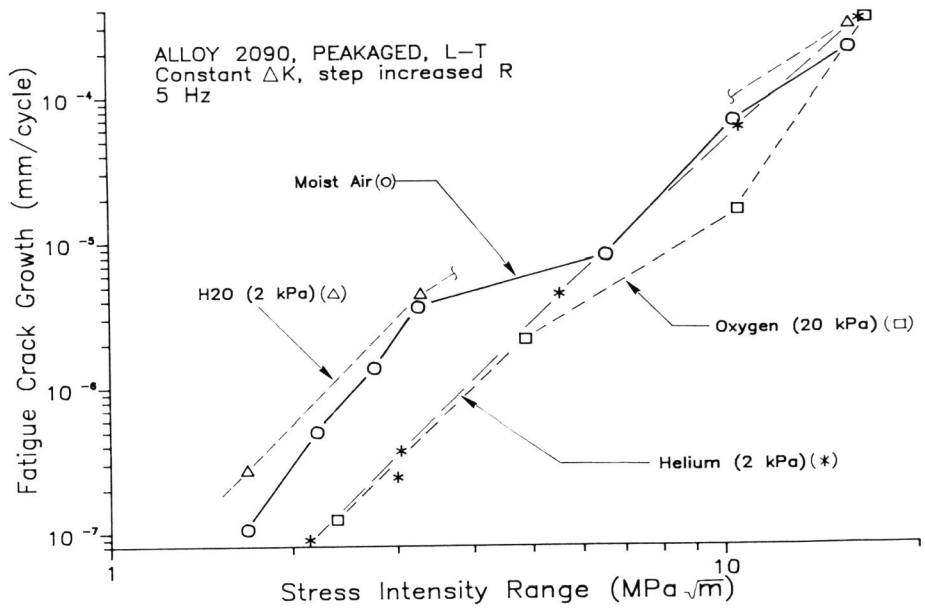

Fig. 3. A comparison of the fatigue crack growth characteristics of alloy 2090 in purified helium, oxygen, water vapor and moist air.

FCG of Alloy 2090 and 7075 in Water Vapor and Helium. Fig. 4 reveals that alloy 2090 generally exhibits a reduced intrinsic fatigue crack growth rate for water vapor compared to 7075. At moderate cyclic stress intensity, crack growth in helium is equivalent for the two alloys. (Note that helium was purified by Method A for alloy 7075 and by Method B for alloy 2090. For moderate ΔK, this difference is not significant based on H_2O pressure-frequency data Gao et al., 1988). Alloy 2090, in 2 kPa water vapor, exhibits similar fatigue crack growth rates compared to helium. A factor of two increase in da/dN is observed for Alloy 7075 in 2 kPa water vapor compared to helium.

For near threshold cracking, fatigue in 7075 for 2 kPa water vapor is significantly faster, a factor of ten, than that observed for 2090. Alloy 2090 exhibits a factor of ten increase in da/dN for 2 kPa water vapor compared to pure helium (Method B), while alloy 7075 exhibits only a slight increase in fatigue crack growth rate for 2 kPa water vapor compared to helium (Method A). Alloy 2090 crack growth rates in the gettered helium environment (Method B) are fifteen times less than those observed for 7075 exposed to cold trap purified helium (Method A). Because of possible helium contamination, the crack growth rate due to mechanical fatigue in 7075 is unknown and the cause for this dramatic effect is unclear.

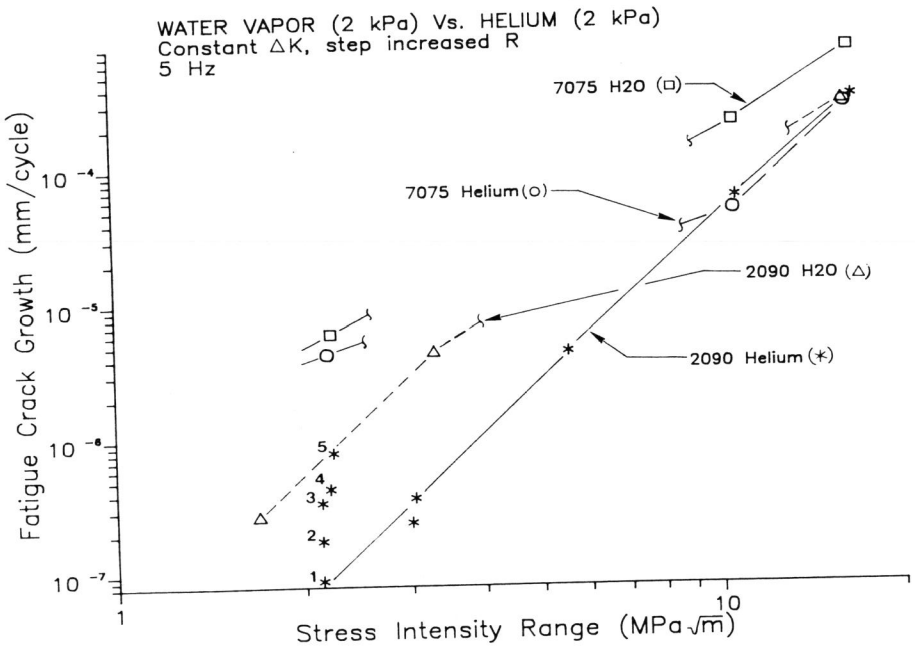

Fig. 4. The fatigue crack growth behavior of alloy 2090 compared to alloy 7075 for water vapor and helium.

A series of near threshold constant ΔK (2.2 MPa·m$^{1/2}$, R=0.88) experiments confirm that small (ppm) levels of H_2O in otherwise pure helium accelerate fatigue crack growth in alloy 2090. Data points 1, 2, and 3 in Fig. 4 represent the sequential measurement of fatigue crack growth rate during a constant ΔK experiment. Point 1 was obtained immediately after helium (Method B) introduction, followed by crack growth rate measurements 2 and 3 as cycling progressed. The fatigue crack growth rate increased by a factor of five, suggesting that environment purity changed during crack growth. After chamber evacuation, the experiment was repeated (data point 4) using cold trap purified helium (Method A), with the wall of the vacuum chamber initially heated for 15 minutes to simulate contaminant outgassing. Data point 4 exhibits an accelerated crack growth rate, similar to point 3 and equivalent to fatigue in moist air. A third experiment, data point 5 in Fig. 4, was performed in pure helium (Method B) containing 3 ppm H_2O. (The chamber was evacuated to 3 μPa, 3 ppm H_2O was added based on capacitance manometer measurement and the chamber backfilled with 2 kPa helium.) The crack growth rate obtained for the 3 ppm (7 mPa) H_2O/helium environment increased 10-fold compared to dry helium, point 1 in Fig. 4, and is similar to the value obtained for the 2 kPa water vapor experiment. The results for alloy 2090 are consistent with results for 7075, Fig. 2 and the findings of Petit and Zeghloul, (1988).

FGC of Alloy 2090 and 7075 in Oxygen and Helium. Results shown in Fig. 5 suggest that oxygen has little effect on the intrinsic fatigue crack growth rate in alloy 2090 compared to purified helium (Method B), particularly near threshold. At moderate ΔK and low R, reduced da/dN (up to a factor of three) is observed for 2090 and 7075 at a ΔK of 10.4 MPa·m$^{1/2}$ (R=0.05) in oxygen compared to helium. These data can be interpreted based on oxide induced closure or surface film effects.

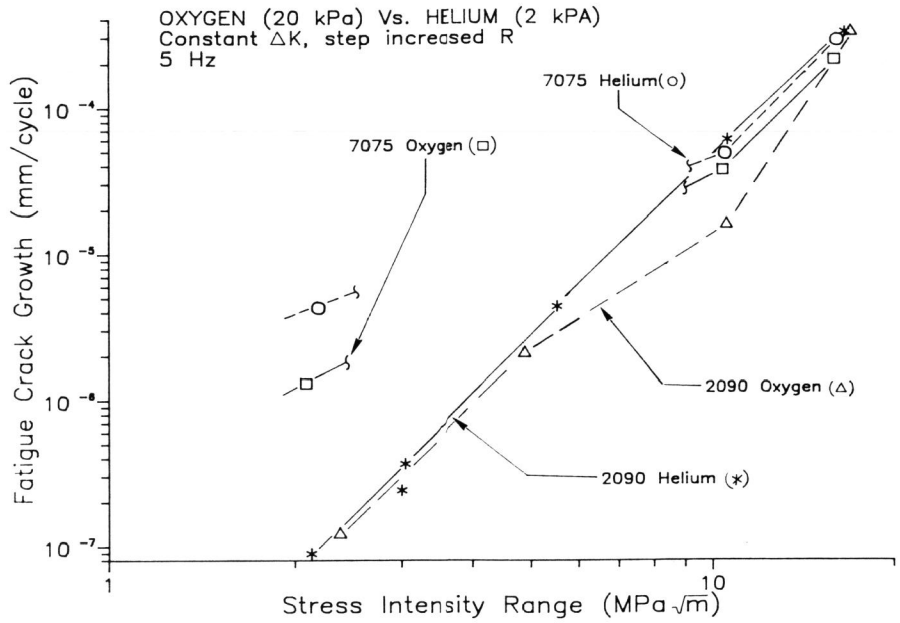

Fig. 5. The fatigue crack growth characteristics of alloy 2090 compared to alloy 7075 for oxygen and helium.

Alloy 2090 crack growth rates at low ΔK and high R for oxygen are comparable to those observed for helium (Method B). Here, alloy 2090 exhibits a factor of ten decrease in intrinsic fatigue crack growth compared to alloy 7075 for oxygen. Presumably oxygen poisons low pressure H_2O environment cracking; the difference in 2090 and 7075 near threshold FCG is thus indicative of a mechanical effect. This speculation will be examined.

Mechanistic Implications

Most studies of environmental fracture of aluminum alloys in gaseous environments containing H_2O conclude that hydrogen, with contributions from dislocation and grain boundary transport, causes embrittlement (Ricker and Duquette, 1988, Gao et al., 1988). Our evidence supports hydrogen embrittlement, particularly near threshold, for transgranular fatigue of Al-Li-Cu alloys. Surface films have a minimal effect on mechanical crack tip damage, but may mitigate hydrogen uptake.

Hydrogen Embrittlement. Water vapor enhanced FCG in aluminum alloys is driven by hydrogen produced through reactions of water vapor with newly created crack tip surfaces (Gao et al., 1988). Because aluminum alloy surfaces react rapidly, the crack growth rate is limited by impeded molecular gas transport to the crack tip. Molecular transport is reduced with decreasing pressure or increasing frequency below a saturation level, resulting in reduced hydrogen production and lower fatigue crack growth rates. Measurements and modeling suggest that the saturation pressure is 5 to 10 Pa for a variety of aluminum alloys loaded at 5 Hz. Environmental embrittlement is eliminated at pressures below about 1 Pa (5 Hz). These trends were established for moderate ΔK, above about 7 MPa$\cdot$m$^{1/2}$ and low R below about 0.1.

Results of corrosion fatigue experiments at moderate ΔK and saturation frequency-H_2O pressure suggest a reduced hydrogen effect in alloy 2090 compared to 7075. Alloy 7075 results are consistent with modeling (Gao et al. 1988) where da/dN in 2 kPa water vapor (saturation) is greater than rates in helium. For alloy 2090, fatigue crack growth rates are similar for the two environments. The difference in behavior for alloys 2090 and 7075 suggests that:

1. The saturation pressure for alloy 2090 is higher due to a rough fracture surface. (Surface roughness impedes molecular transport to the crack tip (Gao et al., 1988)).
2. The limiting coverage at saturation is low for alloy 2090 compared to 7075 due to different surface reactions.
3. Surface reactions in alloy 2090 are slow and rate limiting. Alternately, equal hydrogen forms but less enters alloy 2090 due to surface impedance, viz the formation of lithium hydride or hydroxide.
4. For equal surface hydrogen production, embrittlement is reduced or bulk hydrogen diffusion in alloy 2090 becomes rate limiting.

The precise mechanism is unclear.

Near threshold, extremely low concentrations of water vapor exacerbate FCG in alloys 2090 and 7075. Specifically, data establish a three order of magnitude reduction in the saturation value of H_2O pressure to load frequency ratio. These results reveal a significant extension of the transport controlled crack growth region for alloy 2090 near threshold compared to high ΔK behavior. Increased molecular transport to the crack tip due to increased mean crack opening at high R explains a portion of the reduced H_2O saturation level (Gao et al., 1988). Reduced, but highly localized, crack tip reaction area could also explain the reduction in saturation value at low ΔK. For the moderate ΔK regime, the crack tip contains newly created surfaces, possibly along distributed slip steps, that act collectively as active sites for hydrogen production and subsequent embrittlement. As the cyclic stress intensity is lowered, crack tip damage is localized, possibly along single slip or cleavage planes, reducing the area of active sites. Because of the reduced area, fewer molecules of water vapor are required for coverage and saturation is obtained at a greatly reduced pressure. Even though fewer hydrogen atoms may be produced at the crack tip, the effective hydrogen concentration may not be altered if embrittlement is localized. These speculations are being examined.

Film Effects. Equal fatigue crack growth rates for oxygen and helium at low ΔK in alloy 2090 demonstrate that surface films do not alter crack tip damage by affecting either slip irreversibility or homogenized crack tip

deformation. Surface films are thought to increase fatigue crack growth rates for planar slip materials, particularly age hardened Al alloys, preventing reversible slip (Jata and Starke, 1986). Conversely, surface films could decrease da/dN by homogenizing localized deformation. The lack of an environmental effect of oxygen compared to helium suggests that surface films do not change the mechanical crack tip damage mechanism. Fatigue studies in purified oxygen provide an excellent means of isolating film effects; a tool here-to-fore not exploited.

Alloy 2090 exhibits a slower fatigue crack growth rate in moist air compared to pure water vapor and accelerated da/dN relative to oxygen. Oxygen molecules in moist air competitively adsorb with water vapor, inhibiting the formation of free hydrogen or forming a crack tip surface film that blocks hydrogen entry ahead of the crack tip.

CONCLUSIONS

1. Gaseous environmental effects on FCG in Al-Li-Cu alloy 2090 are significant, particularly near threshold, and are not closure dominated. Growth rates decrease according to the order: water vapor, moist air, helium and oxygen; the latter two cause equivalent da/dN.
2. A hydrogen embrittlement effect is supported by accelerated fatigue crack growth for water vapor. The unexpectedly strong H_2O effect near threshold is attributed to localized crack surface reaction and opening shape.
3. No difference in the intrinsic fatigue crack growth rates for oxygen compared to inert helium indicates that surface films do not influence mechanical crack tip damage mechanisms.
4. Fatigue crack growth rates in moist air are governed by a complex oxygen/hydrogen embrittlement damage mechanism.
5. Alloy 2090 exhibits better intrinsic transgranular environmental fatigue crack growth, and by inference hydrogen resistance, compared to alloy 7075.

ACKNOWLEDGEMENTS

Financial support provided by the NASA-Langley Research Center, grant NAG-1-745 with D.L. Dicus as monitor, is gratefully acknowledged. Alloy 2090 was provided by E.L. Colvin (Alcoa Technical Center), transmission microscopy by W.A. Cassada and experimental assistance by W.C. Porr.

REFERENCES

ASTM E647-88 (1988). "Standard Test Method for Measurement of Fatigue Crack Growth Rates", Annual Book of ASTM Standards, ASTM, Philadelphia, PA, Vol. 03.01.

Cassada, W.A., G.J. Shiflet and E.A. Starke, Jr, (1987). Scripta Met., 21, 387-392.

Crooker, W.A., J.A. Hauser and R.A. Bayles (1987). In: Proc. Conf. Environmental Degradation of Engineering Materials III, M.R. Louthan, Jr., R.P. McNitt and R.D. Sisson, Jr., eds., 521-532.

Gangloff, R.P. (1982). In: Advances in Crack Length Measurement, C.J. Beevers, ed., pp. 175-229, EMAS, UK.

Gao, M., P.S. Pao and R.P. Wei (1988). Metall. Trans., 19A, 1739-1750.

Herman, W.A., R.W. Hertzberg, and R. Jaccard (1988). "A Simplified Laboratory Approach for the Prediction of Short Crack Behavior in Engineering Structures", J. Fatigue and Fracture of Engr. Materials and Structures, in press.

Jata, K. and E.A. Starke, Jr. (1986). Metall. Trans., 17A, 1011-1026.

Lankford, J. and D.L. Davidson (1986). In: Small Fatigue Cracks, R.O. Ritchie and J. Lankford eds., pp. 51-71, AIME, Warrendale, PA.

Petit, J. and A. Zeghloul (1988). "Environmental Influence on Threshold and Near Threshold Behavior of Short and Long Fatigue Cracks", Metall. Trans., in press.

Piascik, R.S. and R.P. Gangloff (1988). "Environment Assisted Degradation Mechanisms in Al-Li Alloys", Report No. UVA/528266/MS88/101, University of Virginia.

Piascik, R.S. and R.P. Gangloff (1988). "Aqueous Environment Effects on Intrinsic Corrosion Fatigue in an Al-Li-Cu Alloy", In: Environment-Induced Cracking of Metals, R.P. Gangloff and M.B. Ives, eds., NACE, Houston, in press.

Ricker, R.E. and D.J. Duquette (1988). Metall. Trans., 19A, 1775-1783.

Saxena, A., S.J. Hudak, Jr., J.K. Donald, and D.W. Schmidt (1978). J. Test. Eval., 6, (3), 167-174.

Venkateswara Rao, K.T., W. Yu and R.O. Ritchie (1988). Metall. Trans., 19A, 549-569.

Yoder, G.R., P.S. Pao, M.A. Inman and L.A. Cooley (1987). In: Competitive Advances in Metals and Processes, Vol. 1, pp. 25-37, SAMPE, Covina, CA.